A major purpose of the Technical Information Center is to provide the broadest dissemination possible of information contained in DOE's Research and Development Reports to business, industry, the academic community, and federal, state and local governments.

Although a small portion of this report is not reproducible, it is being made available to expedite the availability of information on the research discussed herein.

1

LA-UR -86-3785

Los Alamos National Laboratory is operated by the University of California for the United States Department of Energy under contract W-7405-ENG-36

LA-UR--86-3785

DE87 002918

TITLE CONVECTIVELY DRIVEN SUPERFLUID TURBULENCE IN DILUTE SOLUTIONS OF ^{3}He IN SUPERFLUID ^{4}He

AUTHOR(S) Robert E. Ecke, Hans Haucke and John Wheatley

SUBMITTED TO Proceedings of the Conference on Quantum Fluids and Solids 1986 held in Banff, Canada, October 13-17, 1986

DISCLAIMER

Los Alamos Los Alamos National Laboratory
Los Alamos, New Mexico 87545

FORM NO 836 R4
ST NO 2629 5/81

MASTER

DISTRIBUTION OF THIS DOCUMENT IS UNLIMITED

CONVECTIVELY DRIVEN SUPERFLUID TURBULENCE IN DILUTE SOLUTIONS OF ^{3}He IN SUPERFLUID ^{4}He

Robert E. Ecke, Hans Haucke[†], and John Wheatley[*]

Los Alamos National Laboratory

Los Alamos, New Mexico

Abstract

A dilute solution of ^{3}He in superfluid ^{4}He usually behaves as a single component classical fluid in the context of hydrodynamic convection. However, certain convective states can be excited which do not seem to exist in classical convection. These states are characterized by noisy temperature fluctuations and a pronounced decrease in thermal conductance relative to the classical convecting states. Critical convective flow fields are observed analogous to critical velocities for superfluid turbulence in pipes. The magnitude of the average critical velocities for these two types of superfluid turbulence are in good agreement. Also, a quantitative estimate of energy dissipation due to the interaction of normal fluid and quantized vortex lines appears to account for the large decrease in thermal heat transport for the turbulent states. These states are identified as states of convectively driven superfluid turbulence.

Introduction

Convection in dilute solutions of ^{3}He in superfluid ^{4}He has proven to be an excellent system for the study of classical nonlinear dynamical phenomena. Theoretically[1,2] these mixtures are expected to undergo classical single component convection similar to a fluid such as water. Experimentally, a large amount of work, in particular studies of behavior in the vicinity of the transition to oscillatory convection[3,4] and detailed experiments on quasi-periodicity and mode-locking,[5] supports this theoretical point of view. However, the theoretical treatment ignores quantum vortex line excitations of the superfluid. Examples of thermally driven superfluid hydrodynamics in long pipes show clear evidence for energy dissipation via the interaction of quantum vortex lines and the normal fluid. This type of superfluid turbulence is typically observed in thermal counterflow experiments involving pure HeII although one also sees dissipative phenomena in pure superflow at low temperatures.[6] It has also been shown experimentally[7] that vortex lines are always present in pure HeII, presumably pinned to the walls of the container. As normal fluid velocity is increased vortex lines can be depinned and subsequently stretched by interactions with the normal fluid. A steady-state develops as the generation of vortex line by the flow is balanced by annihilation at the walls.[8] In dilute solutions of ^{3}He in superfluid ^{4}He counterflow is difficult to realize due to the coupling of the normal ^{4}He fraction to the ^{3}He impurities. Thus superfluid turbulence has not been studied for solutions. However, convection in dilute solutions produces a net velocity field of normal fluid (normal ^{4}He and ^{3}He) which can interact with the virtually stationary superfluid. We observe states whose properties can only reasonably be explained as arising from just such an interaction. The

resulting system is one where states exhibiting nonlinear behavior and turbulent flow (temporal chaos) due to classical friction can coexist with states whose properties are dominated by the interaction of normal fluid and vortex lines.

As noted above, convection in dilute solutions of ^{3}He in superfluid ^{4}He in the absence of superfluid excitations can be described by the same parameters as for classical convection.[1] The first of these dimensionless parameters is the Rayleigh number, defined as

$$R \equiv g\alpha d^3 \Delta T/\upsilon\chi, \qquad (1)$$

where g is the acceleration due to gravity, α is the effective thermal expansion coefficient, d is the cell height, ΔT is the temperature difference across the fluid layer, υ is the kinematic viscosity and χ is the thermal diffusivity. Below some critical value of R (R_c = 1706 for a laterally unbounded fluid layer[9]) heat is conducted diffusively and there is no fluid motion. For $R > R_c$ fluid is conducted both diffusively and via the convective fluid motion. One measures heat transport by dividing the applied heater power by the observed temperature difference. In the diffusive regime, this is just a constant, namely the thermal conductance, K_c. As convective motion of the fluid begins there is enhanced heat transport and a measured thermal conductance K which is greater than K_c. The Nusselt number is defined as the ratio K/K_c and is a measure of the enhancement of heat transport; Nu is identically one in the diffusive regime and takes on values greater than one for the convective state. Close to onset Nusselt should increase linearly with R/R_c.[9]

The other important dimensionless parameter, which together with the Rayleigh number and the cell geometry completely characterizes the convective

state, is the Prandtl number σ. The initial transition to the convective state does not depend on σ but instabilities at higher Rayleigh number are strongly dependent on σ. The Prandtl number is the ratio of kinematic viscosity υ and thermal diffusivity χ and is a measure of the ratio of relaxation time for heat to that for vorticity. The dilute solutions have a low Prandtl number which varies in the range $0.04 < \sigma < 0.15$ for temperatures in the range $0.6 < T < 1.5$ K. Thus heat is diffused rapidly relative to vorticity and the secondary instabilities are primarily time-dependent as opposed to instabilities to more complex time-independent fluid flows.[10] The transitions to time dependence observed in our system have been the object of intense study but are not reported here. Details can be found elswhere.[3,4,5] For data presented here with a bottom plate temperature of 0.85 K and 1.46 % ^{3}He atomic concentration, the Prantl number is 0.066.

Experiment

The convection cell, figure 1, consists of copper top and bottom boundaries, a stainless steel can to confine the fluid and a thermally insulating spacer made from a commercially available graphite-loaded polymide resin,[11] which defines the actual region for convective fluid flow. The dimensions of the this rectangular region are 0.8 cm (high) x 1.6 cm x 1.12 cm. The cell geometry can be modified simply by replacing the spacer. Temperatures on the top and bottom plates are measured with calibrated germanium resistance thermometers. The bottom plate temperature is regulated to ± 5 μK and heat is introduced, via an electrical resistance heater, to the top plate owing to the effectively negative expansion coefficient of the solutions.[1,4] This negative expansion coefficient arises from a small (about 10^{-5} cm/sec) counterflow

velocity which carries ^{3}He impurities away from the warmer surface. The resulting ^{3}He concentration gradient is gravitationally unstable due to the lower density of ^{3}He relative to ^{4}He. The heat flow into the top plate is conducted through three parallel paths: the stainless steel can, the insulating spacer and the fluid itself. The contribution of the can and spacer to the total heat flow is about 15% at 0.85 K. In addition there is Kapitza boundary resistance between the fluid and the boundaries which accounts for about 5% of the total temperature difference across the cell at 0.85 K. Both of these effects were measured and the data corrected accordingly.

The primary probe of time-dependent fluid motion in the cell is a local thermocouple which measures temperature differences between a thermally insulated copper plug and the top plate. The temperature differences arise from differential heat flows into the plug and the top plate. The thermocouple consists of a piece of gold + 0.03 atm. % iron wire with niobium leads connected to a SQUID ammeter.[12] The sensitivity of this probe is about 0.3×10^{-7} K/ $\sqrt{\text{Hz}}$. The probe area is only 3.8% of the top plate area exposed to the fluid and does not significantly affect the fluid flow except in the vicinity of the convective onset. In that region the small distortion of the boundary conditions due to the probe can selectively excite different convective states depending upon the fraction of total power applied to the probe heater. This is an important point and will be discussed in more detail below.

Data

Observations in convecting dilute solutions of ^{3}He in superfluid ^{4}He of noisy states close to the convective onset, characterized by greatly reduced

heat transport efficiency relative to quiet states, were first made by Haucke et al.[13] The origin of these states was not clear at the time and only later[4] was the speculation put forward that the explanation could be quantized vortex line excitations in the superfluid. During the last several years we have accumulated qualitative observations as well as precise heat flow data which lend credence to that speculation. The qualitative observations are related to the stability of the noisy states. Before discussing these observations in detail we present the heat transport data by which these states were first identified. Figure 2 shows the Nusselt number for six different states plotted as a function of R/R_c where $R_c \approx 2000$ is the critical Rayleigh number. The three states with highest Nu are time-independent states (static velocity field) with probe temperature fluctuations which are just the instrumental noise. In comparison the noisy states are characterized by temperature fluctuations at the probe many times the instrumental noise. Figure 3 illustrates the difference between a time series of a quiet state and that of a noisy state at $R/R_c \approx 1.6$ as measured by the probe thermocouple. All three noisy states have similar large amplitude fluctuations and decreased Nusselt relative to the quiet states. The merging of the quiet and noisy branches of Nusselt number as seen in Fig. 2. is a very important feature of the data not observed in previous work[4,13] and is discussed in detail below. The Rayleigh number where the branches come together is denoted R_n.

Observations of the stability of the quiet and noisy branches are important in interpreting the data. The transition from a quiet to a noisy state is usually induced by a mechanical or thermal disturbance although spontaneous transitions can also occur. Transitions from a noisy state to a quiet state are never observed. The probability of a spontaneous transition

is very history dependent; a short time following the initial cooldown or after the system has been left in a noisy state for some time the probability is high. If the system remains in a quiet state for long periods or if the fluid is "annealed" by warming above the lambda point and then cooling very slowly the probability for a spontaneous transition is greatly reduced. In fact if the system remains in a quiet state too long, say several weeks, it is sometimes impossible to get the noisy states at all. Even the application of strong mechanical disturbances fails to induce the noisy state and one must warm above the lambda point and cool rapidly in order to again be able to induce the noisy states. The value of R at which a spontaneous transition occurs is not reproducible and is also history dependent in a similar manner as above; the longer the system is in a quiet state the higher the value of R at which a transition will occur. An interesting exception to this statement is that if the quiet state becomes time-dependent as for example when a periodic temperature oscillation occurs as measured by the probe, spontaneous transitions to the noisy state will not occur even for much higher values of R (mechanically induced transitions still occur). Why the time-dependent motion of the fluid stabilizes the quiet state against spontaneous transitions to the noisy state is not presently understood.

The three quiet states with different Nusselt probably correspond to different configurations of the flow field. From numerical simuations[14] and experiments using other fluids in similar cell geometries[15] the three states can be identified with the following roll states: two parallel rolls with roll axis perpendicular to the longer lateral side and fluid rising in the center, the same roll structure but with fluid falling in the center, and one roll with the roll axis parallel to the longer lateral side. We label these three

states as 2r↑, 2r↓ and 1r to denote two-roll-center-fluid-rising, two-roll-center-fluid-falling, and one roll states respectively. The 2r↑ and 2r↓ states are symmetric states (under the operation of reversing the sign of the velocity) and thus should have the same heat transport effeciency. Figure 2 shows that aside from some small differences attributable to experimental conditions the two states are identical in Nusselt number. Therefore, heat transport alone is inadequate to uniquely identify the states.

The different roll states can be unambigously distinquished by their influence on the probe thermocouple. The two roll states 2r↑ and 2r↓ give large temperature responses with opposite sign due to the colder fluid (2r↑) or warmer fluid (2r↓) being concentrated on the probe due to the vertical flow of the fluid in the two roll states. The one roll state on the other hand does not give a strong response since the fluid is generally flowing horizontally across the probe for that state and the net response is averaged out. Figure 4 shows the probe thermocouple response for the three quiet states and also for the noisy states. It is clear from this data that each noisy state is directly associated with one of the quiet branches and that the perturbations which cause the large decrease in heat transport effecieny do not change the gross roll structure of the fluid flow. Thus we label the noisy states as $2r\uparrow_n$, $2r\downarrow_n$, and $1r_n$ to denote the noisy counterparts to the quiet states. Note that as for the quiet states, the symmetric noisy states have nearly the same Nusselt dependence on R (see Fig. 2) and that the one roll noisy state has lower Nusselt number relative to the two-roll noisy states.

The fact that there are three different roll structures which we can detect raises the question about how each state is created. The answer to this question lies in the construction of the local probe situated in the top

plate. The probe area represents about 3.8% of the total top plate area exposed to the fluid. There is an electrial resistance heater attached to the probe which allows heat to be applied to the probe. When no power is applied to the probe heater, but the total heater power is positive, the probe remains slightly cooler than the rest of the top plate. With this perturbed boundary condition, the most stable state is the 2r↑ state which is reasonable since the cold singularity of the probe should favor the colder fluid rising in the center. Alternately, by applying power to the probe greater than the geometric ratio of probe to total top plate area, 3.8%, the probe is made warmer than the top plate and the 2r↓ state is excited. For heater power ratios close to 3.8% the one roll state is excited. The procedure for selecting different states is to begin below the convective onset with a probe heater power appropriate for the desired state. As R is increased above R_c, through increases in the total heater power, the desired state is selected and the system remains in that state even when the probe power is changed. After reaching some value of $R > R_c$ the probe heater power is adjusted to the geometric ratio of probe to top plate area so as to most closely duplicate ideal boundary conditions. All data are thus taken with decreasing rather than increasing R. Another consequence of this method is that very close to onset the selected state becomes unstable with respect to the one roll state and discontinuous changes can be observed in both Nusselt number, Fig. 2., and probe amplitude, Fig. 4. The noisy analogs of the quiet states are created by first preparing the quiet state and then inducing a transition to the noisy state by the application of a mechanical disturbance. For bottom plate temperatures of 0.70 K and 0.85 K, one always gets the analog noisy state from the prepared quiet state and transitions from one noisy state to another are

not observed. However, at 0.95 K, the noisy states are not as stable and transitions can occur. The systematics of these transitions has not been studied as yet. If the Rayleigh number is decreased below R_n (the point at which the Nusselt curves merge, Fig. 2), but still above R_c, the system will remain in the quiet state even if R is again increased above R_n.

Another feature of the noisy state is its spectral content as revealed by a Fourier transform of the digitized output of the probe thermocouple. Figures 5a and 5b illustrate power spectra for the $2r\uparrow_n$ and $1r_n$ noisy states respectively. The primary features of these spectra are the low frequency plateau and rolloff at high frequencies. Although the high frequency portions of the power spectra appear to obey a power law rolloff, the exponent of that power law seems to increase continuously as R is increased; values between 2 and 6 have been observed. The total power in the noisy fluctuations decreases as one decreases R and approaches the background noise floor just at R_n. Although there does not seem to be much quantitative difference between the total rms amplitudes for the different noisy states, there is a broad low frequency peak which appears in power spectra of the $1r_n$ state, Fig. 5a) but not for the two roll noisy states, Fig. 5b). The origin of this feature may be due to a transition of the quiet state roll to a time dependent oscillation which is broadened by the presence of the noisy fluctuations. However, the frequency of the low frequency peak, about 0.1 Hz, is appreciably less than the oscillatory frequency, about 0.5 Hz, for the quiet state and thus that identification is not very clear.

Interpretation

The interpretation of the data is based on the hypothesis that quantized

vortex line excitations of the superfluid are present in the solutions and that at sufficiently large convective flow fields these excitations become depinned from the surface, interact with the normal fluid fraction and generate the phenomenon known as superfluid turbulence. The experimental observation that a mechanical disturbance is often necessary to create the noisy state is consistent with that picture; the energy needed to depin a vortex line must then be quite high. It must also be true that the vortex line distribution relaxes with a very long relaxation time from a moderate value following a cooldown or after having been in a noisy state, to a small value if left undisturbed in a quiet state. This would explain why it becomes harder to induce the noisy state and why the probability of spontaneous transitions decreases with time. The merging of the Nusselt number branches shown in Fig. 2 is consistent with experimental observations and theoretical interpretations of superfluid turbulence in pure HeII that there is a critical velocity above which a nucleated vortex tangle can grow and be self-sustaining.[6,15] Hysteresis also exists in those experiments since the velocity at which the vortex tangle fails to be sustained by the fluid flow may be appreciablely less than the nucleation velocity. In the convection data presented here it appears that the nucleation energy can be very high relative to that in straight channels since one can achieve very much larger hysterysis regions. For example, we have reached values of $R/R_c \gtrsim 10$ without observing a transition to the noisy state.

The large decrease in heat transport efficiency of the noisy states relative to the quiet states could conceivably be due to changes in the fluid parameters brought about by the presence of a vortex tangle. One can rule out changes in the heat capacity since the vortex line energies are small.[16]

Changes in transport coefficients (thermal conductivity, viscosity and thermal expansion) should also be small since estimates suggest that scattering of quasiparticle excitations is much more probable than quasiparticle-vortex-line scattering. However, the effective thermal conductivity contains both diffusive and counterflow contributions.[1] The latter contribution could be affected by the presence of quantized vortex lines. We do not have any way of calculating the size of this effect so it remains as a possible candidate to explain the decrease in heat transport efficiency observed for the noisy state. However, as we will see below another mechanism is capable of accounting for the Nusselt number decrease.

The decrease in heat transport can be explained by assuming that extra energy is being dissipated by the interaction of vortex lines and normal flow and consequently the fluid velocities are smaller and the Nusselt number reduced. To make this comparison quantitative we compare estimates for the force density due to the mutual friction force between normal fluid and vortex lines with the buoyant force density driving the convection. The buoyant power is given by $P_\alpha = \rho g \chi(-\alpha \Delta T)(Nu - 1)A$ where ρ is the fluid density, g is the acceleration of gravity, α and χ are respectively the thermal expansion coefficient and the thermal diffusivity, and A is the cross sectional area of the cell. To obtain a force density we divide P_α by the cell volume and an average convective velocity v which yields $f_\alpha = \rho g \chi(-\alpha \Delta T)(Nu - 1)/dv$. For the mutual friction force density we use the phenomenological Gorter-Mellink equation,[17] an empirical expression describing superfluid turbulence in thermal counterflow experiments:

$$f_{ns} = \xi \rho_s \rho_n \cdot v_{ns}^3 \qquad (2)$$

where ξ is an empirical constant, ρ_s and ρ_n are the superfluid and normal

fluid densities respectively, and v_{ns} is the relative velocity of the normal and superfluid fractions. To evaluate Eq. 2 for dilute solutions we use the expression $\rho_n = \rho_{n4} + \rho c m^*/m_3$,[4] where m^* is the effective mass of a ^{3}He quasiparticle,[18] c is the mass fraction of ^{3}He, and ρ_{n4} is the contribution of the ^{4}He excitations to the normal fluid density. For the dilute solution used in this work, x = 1.46 %, and for a temperature of 0.85 K, we have ρ_n/ρ = 0.028. Values for ξ in pure HeII range from about 10 to 100 cm-s/g over the temperature range 1.2 to 2.0 K. If we take a temperature such that the normal fluid fraction of HeII is equal to the normal fluid concentration in our solution we get 1.2 K and a value of ξ = 10 cm-s/g. An alternate approach to estimating an effective ξ value is to examine recent results on flow of ^{3}He in superfluid ^{4}He at very low temperatures, less than 150 mK, in a dilution refrigerator.[9] An effective Gorter-Mellink equation is obtained but with a variable power law dependence on velocity with an exponent between 2.4 and 3.2 as opposed to the value 3 used in Eq. 2. Using a microscopic theory due to Schwarz[20] which relates ξ to the mutual friction coefficient we extrapolate their result to our densities and obtain limits $10 < \xi < 50$ cm-s/gm for exponent values between 2.6 and 3.0. We use $\xi \approx 25$ cm-s/g and obtain f_{ns} = $1.5 \times 10^{-2}\ v_{ns}^3$ dynes/cc. Clearly we can only make order of magnitude estimates. To evaluate the expressions for f_α and f_{ns} we need an estimate of the average convective velocity. By balancing the loss of kinetic energy due to viscous drag against the gain arising from buoyant forces gives a relation between Nusselt number and an average velocity v:

$$(vd/\chi)^2 = C\cdot(Nu - 1) \qquad (3)$$

where C is a constant of proportionality. Numerical work of Clever and Busse[9] agrees well with Eq. 3 and yields values of $40 \leq C \leq 75$ for Prandtl numbers in

the range $0.01 \leq \sigma \leq 0.7$ and $\epsilon \equiv R/R_c - 1$ between 0 and 1. We use the value C = 60 but note that using other values of C in the range consistent with the numerical work would not change the estimates of velocity by more than 30 %. We want to evaluate the contributions to the force densities in the vicinity of the onset so we use $R/R_c = 1.4$ for which $Nu - 1 \approx 0.1$ (see Fig. 2). This gives $v \approx 0.24$ cm/s for the average convective velocity. With that value of velocity and assuming $v_{ns} \approx v$, expressions for f_{ns} and f_α yield values of 2×10^{-4} dynes/cc and 3×10^{-4} dynes/cc respectively. Although the estimate for the mutual friction force density assumes that $v_{ns} \approx v$ and is thus an upper bound on f_{ns}, the order of magnitude agreement suggests that extra energy dissipation due to the interaction of vortex lines and normal fluid could account for the large decrease in Nusselt number between the noisy and quiet convecting states.

Another quantitative estimate which adds credence to our stated hypothesis regarding vortex line excitation is a comparison of critical velocities for our convecting system and for thermal counterflow superfluid turbulence in long narrow channels. In the latter case the critical velocity can vary considerably with the cross sectional area of the channel.[6] However, by scaling the results by a mean diameter D, one obtains scaled critical velocities in the range $0.05 < v_c D < 0.13$ cm^2/s. This is to be compared with scaled critical velocities from the convection work at different bottom plate temperatures using the Nusselt number evaluated at R_n, see Fig. 2, in Eq. (3) to evaluate the velocities. We scale these velocities by the cell height d and obtain values for the scaled critical velocities $0.11 < v_c d < 0.14$ cm^2/s for $0.7 < T < 0.95$ K. Although this comparison is for different fluid systems and different temperature regimes (the normal fluid fractions are quite close

however) the order of magnitude agreement is quite satisfying.

One last point of comparison between superfluid turbulence in the convective system and in the long channel configurations is the power spectral signature of the noisy fluctuations for both systems. Power spectra for the convective case, Figs. 5a,b, are obtained from Fourier transforms of the digitized output of the probe thermocouple. In the counterflow experiments power spectra are obtained from direct measurements of vortex line density,[6,21] and from temperature difference measurements and chemical potential.[22] The power spectra so obtained are all very similar, showing a low frequency plateau and high frequency rolloff with varying power law dependences. Early measurements in the counterflow experiments[6,21], indicated increasing total power in the fluctuations as the heat flow through the channel was increased (for induced relative velocities above the critical velocity). Similarly, we observe a steady increase in total rms power for the noisy states as the Rayleigh number is increased above R_n. However, recent results due to Tough et al.[22] suggest that for counterflow experiments fluctuations (in temperature at least) are the result of noise amplification near the second critical transition and are only large in the vicinity of that transition; decreasing in magnitude both above and below that point. We do not observe any analogous effect in our convecting system, but that may be due to the different nature of turbulent flow in convection and in pipe flow; the critical Reynolds number in pipe flow is well known to depend on the conditions of the pipe on the input side.

Conclusions

The phenomena which we observe in our convecting dilute solution of ^{3}He

in superfluid ^{4}He are consistent with the hypothesis that quantized vortex line excitations of the superfluid are present in our convection cell, are depinned due to mechanical disturbances or occasionally spontaneous processes, and in the presence of normal fluid motion create a vortex tangle. This vortex tangle is stable provided the normal fluid velocity is greater than some critical value and gives rise to decreased heat transport in the noisy states because of the energy dissipation arising from the mutual friction force between superfluid vortex lines and the normal fluid. Quantitative estimates of energy dissipation and critical velocities are in agreement with this picture. According to the hypothesis, the temperature fluctuations observed for the noisy states are due to the stochastic competition of regeneration of vorticity due to the mutual friction forces and annihilation of vortex lines at the walls of the container.[23] Although this view is entirely consistent with the data and with the fact that no other convection experiments on classical fluids in small aspect ratio cells have observed such states, direct measurement of vortex line densities utilizing second sound or ion trapping probes would be an important verification of the picture.

Acknowledgements

This work was supported by funds provided by the Department of Energy, Office of Basic Energy Sciences, Division of Materials Science. We would like to acknowledge valuable discussions with J. Tough, G. Baym, A. Libchaber, and K. Schwarz.

References

† Present address: IBM T.J.Watson Research Center, Yorktown Heights, NY 10598.

* Deceased March, 1986.

1. A. Fetter, Phys. Rev. B26, 1164 and 1172 (1982).

2. V. Steinberg, Phys. Rev. A24, 975 (1981).

3. Y. Maeno, H. Haucke, and J.C. Wheatley, Phys. Rev. Lett. 54, 340 (1985) and R.E. Ecke, Y. Maeno, H. Haucke, and J.C. Wheatley, Phys. Rev. Lett. 53, 1567 (1984).

4. Y. Maeno, H. Haucke, R.E. Ecke, and J.C. Wheatley, J. Low Temp. Phys. 59, 305 (1985).

5. R.E. Ecke, H. Haucke, and J.C. Wheatley, in "Perspectives in Nonlinear Dynamics," ed. by M.F. Shlesinger, R. Cawley, A.W. Saenz, and W. Zachary, (World Scientific Publ., Sinapore, 1986) p.84 and H. Haucke and R. Ecke, accepted for publication in Physica D.

6. For an excellent review of experimental properties of superfluid turbulence see J. Tough, in "Progress in Low Temperature Physics," Vol. VIII, ed. by D. Brewer (North Holland Publ. Co., Amsterdam, 1982) ch. 3.

7. D.D. Awschalom and K.W. Schwarz, Phys. Rev. Lett. 52, 49 (1984).

8. K. Schwarz, . . . ???

9. R. Clever and F. Busse, J. Fluid Mech. 65, 625 (1974); J. Fluid Mech. 102, 61 (1981).

10. F. Busse, Rep. Prog. Phys. 41, 1929 (1978).

11. Vespel is manufactured by Dupont Co., Wilmington, Delaware 19898; For low-temperature thermal conductivity see M. Locatelli, D. Arnaud, and M. Routin, Cryog. 16, 374 (1976).

12. Y. Maeno, H. Haucke, and J. Wheatley, Rev. Sci. Instrum. 54, 946 (1983).

13. H. Haucke, Y. Maeno, P. Warkentin, and J.C. Wheatley, J. Low Temp. Phys. 44, 505 (1981).

14. B. Edwards, unpublished.

15. Old experiments see Yoshi these and JLTP.

16. D. R. Tilley and J. Tilley, "Superfluidity and Superconductivity," (John Wiley and Sons, New York, 1974).

17. C. F. Barenghi, R. J. Donnelly, and W. F. Vinen, J. Low Temp. Phys. 52, 189 (1983).

18. R. Radebaugh, National Bureau of Standards Technical Report No. 362 (U.S. Government Printing Office, Washington, 1967).

19. C. A. M. Castelijns, J. N. M. Knerten, A. T. A. M. de Wuele and H. J. Crissman, Phys. Rev. B 32, 2870 (1985).

20. K. N. Schwarz, Phys. Rev. Lett. 49, 283 (1982).

21. C. W. Swmith, Proc. 17th International Conference on Low Temperature Phys., U. Echem, A. Schmid, W. Weber, and H. Wuhl, eds. (Elsevier Science Publ. B. V., 1984).

22. J. Tough, private communication.

23. J. A. Northby, Phys. Rev. B 18, 3214 (1978); see Smith paper.

Figure Captions

Fig. 1. Detail view of convection cell.

Fig. 2. Nusselt number vs. R/R_c. The 2r↑ (+) and 2r↓ (x) quiet branches have very similar Nusselt numbers as do the noisy analog states, 2r↑n ( ) and 2r↓n (Δ). The symbols are roll states 1r and $1r_n$ are • and , respectively. At R_n the noisy branches merge with the quiet branches, and some rounding of the transition from noisy to quiet is visible.

Fig. 3. Temperature fluctuations for quiet state (a) and nosiy state (b) measured by the probe thermocouple. R/R_c 1.6. In the case of the quiet state, noisy is purely instrumental.

Fig. 4. Plot of average probe tempreature vs. R/R_c for various states at a bottom plate temperature of 0.85 K. a) coarse scale, b) big resolution near the convective onset. The +, •, and x symbols denote the 2r↑, 1r and 2r↓ states respectively. The symbols , and Δ denote the $2r\uparrow_n$, $1r_n$ and 2r↓n noisy states respectively.

Fig. 5. Power spectra for two noisy branches at a bottom plate tempe.ature 0.85 K. The spectra have been smoothed with a sliding boxcar having a width of 0.1 $\log_{10}$ (Hz). A frequency independent noise background of -68.8 dB is subtracted from the data.

a) Spectra for the $1r_n$ noisy state. From top to bottom, the $1R_c$ values are 9.015, 2.793, and 1.45a.

b) Spectra for the 2r↑n noisy state. From top to bottom, the R/R_c values are 6.969, 3.61, 2053 and 1.571.

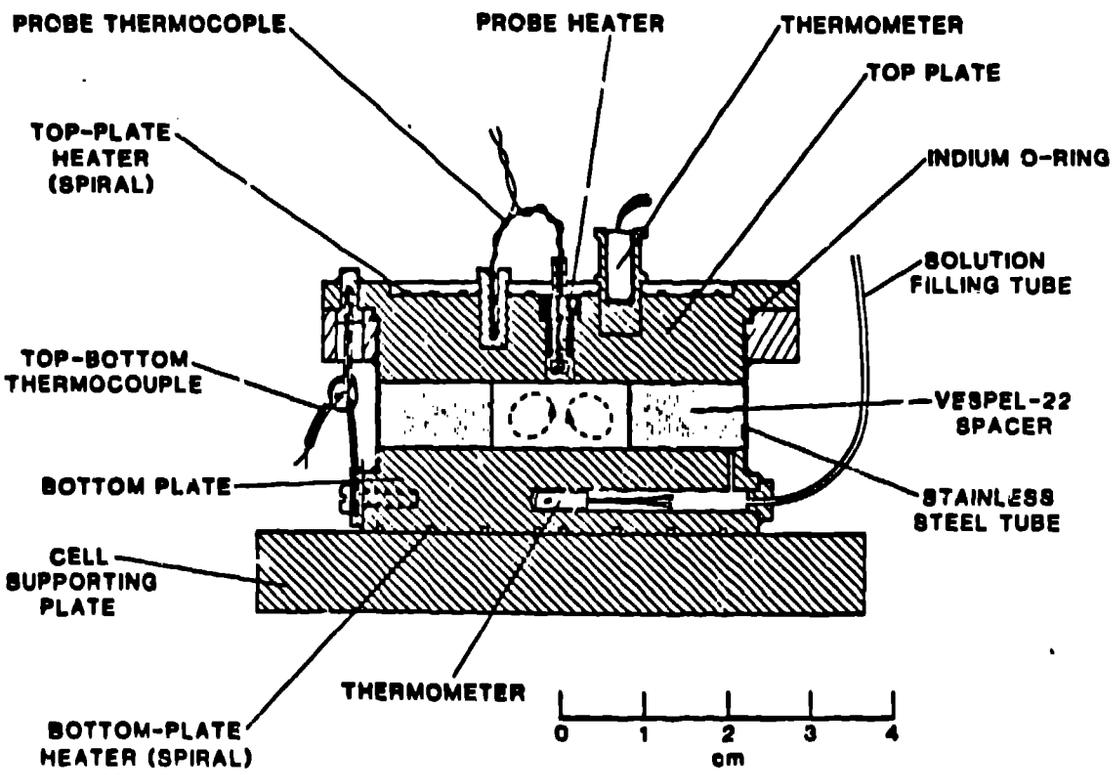

Fig. 1. Detail view of the cell.

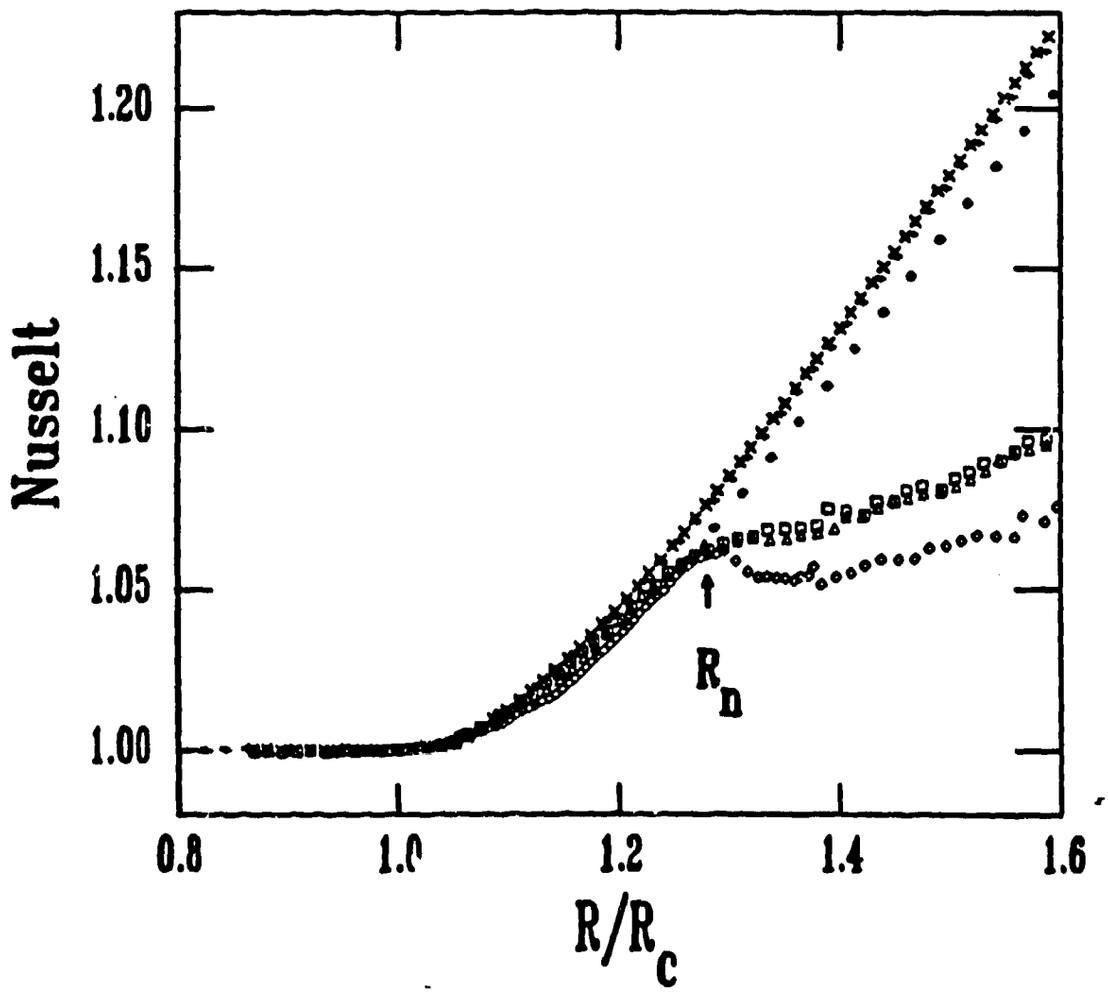

FIG 2

FIG 1

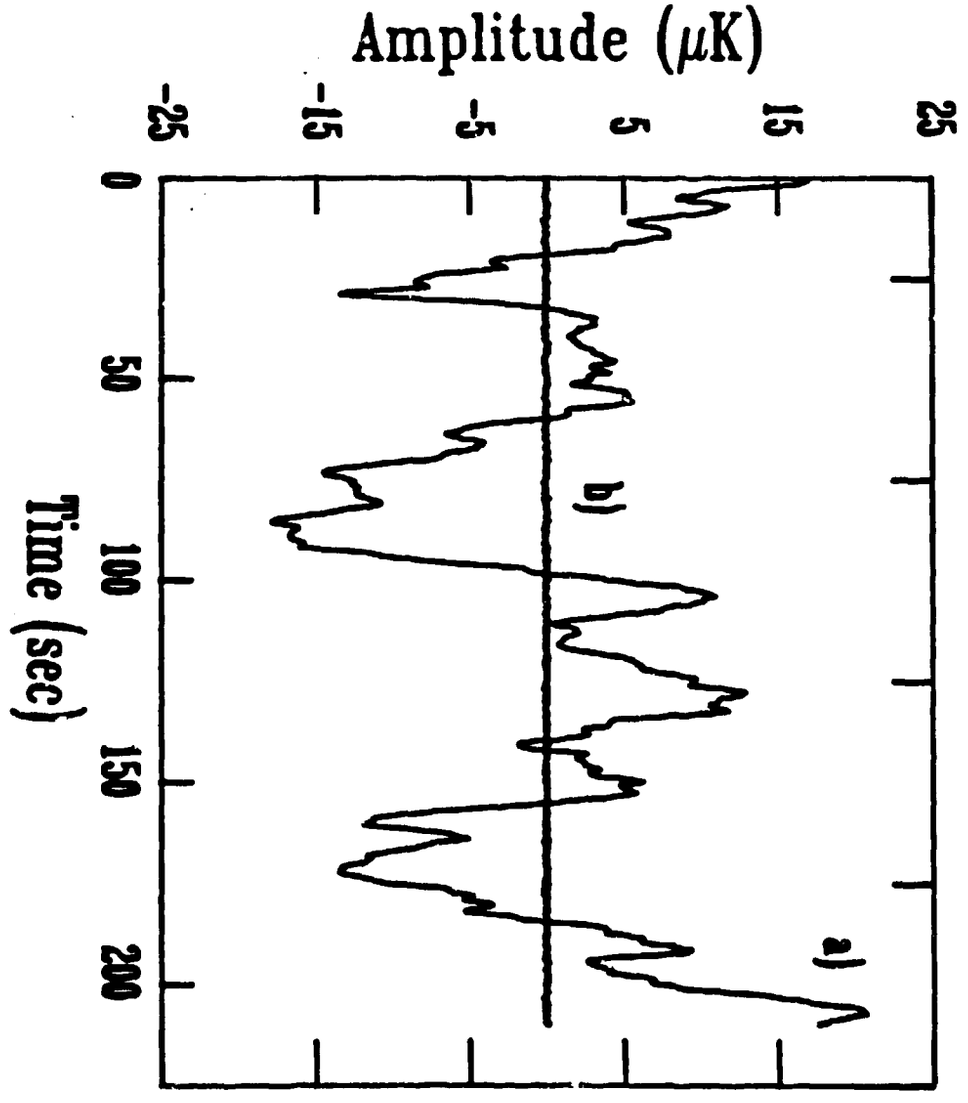

FIG 3

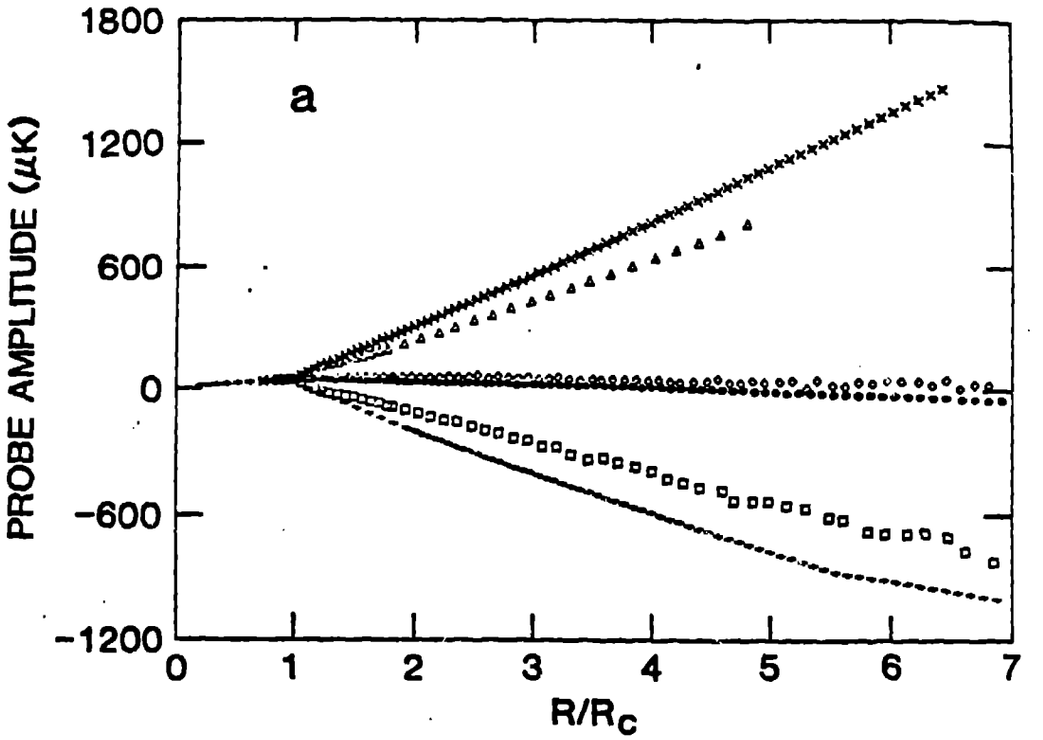
a
1800
1200
600
0
-600
-1200
PROBE AMPLITUDE (μK)
0
1
2
3
4
5
6
7
R/Rc

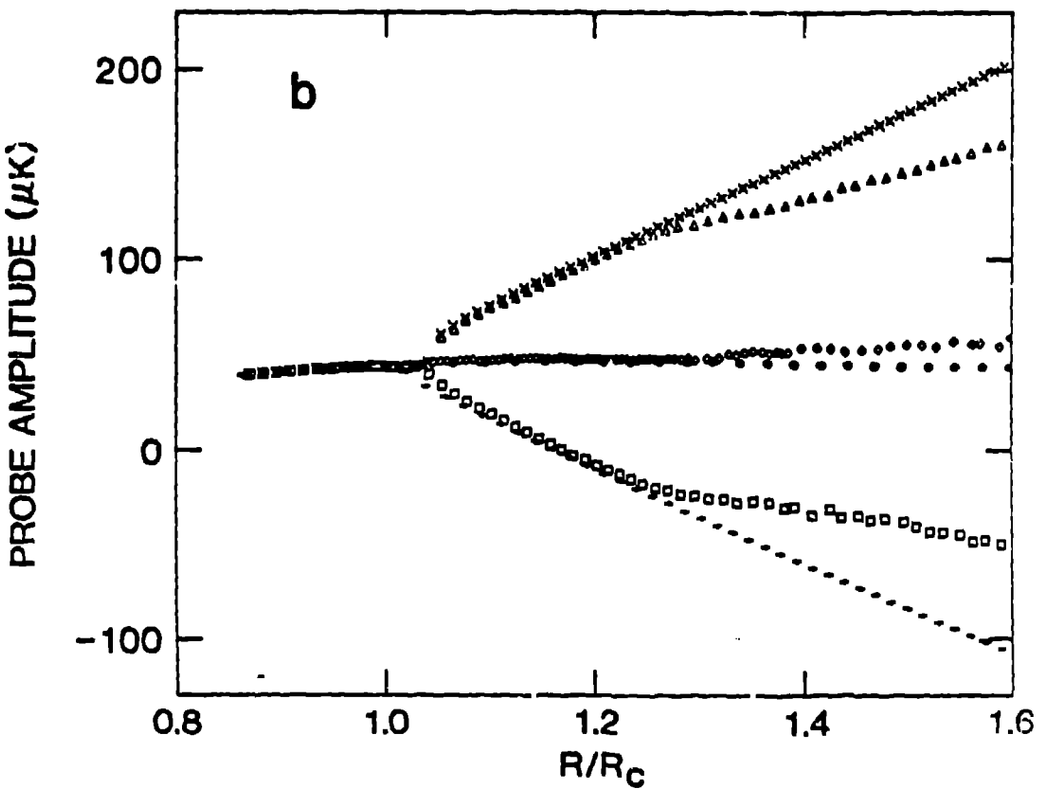
b
200
100
0
-100
PROBE AMPLITUDE (μK)
0.8
1.0
1.2
1.4
1.6
R/Rc

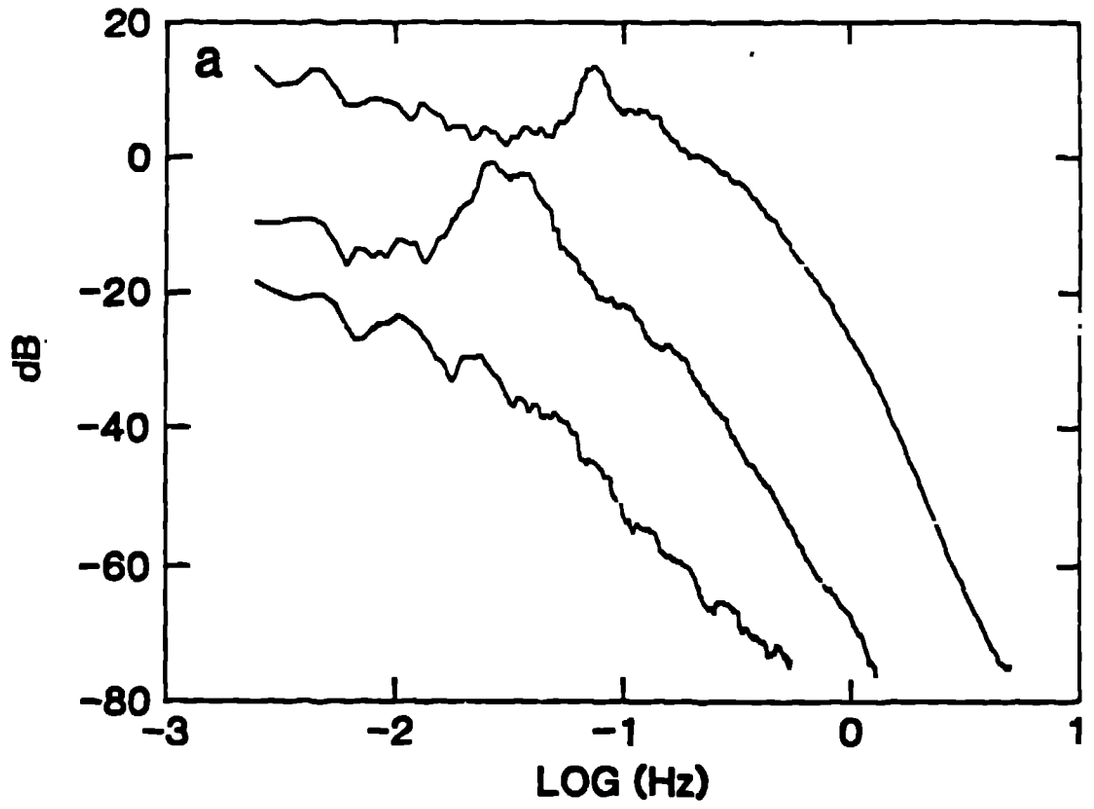
a
20
0
-20
-40
-60
-80
dB
-3
-2
-1
0
1
LOG (Hz)

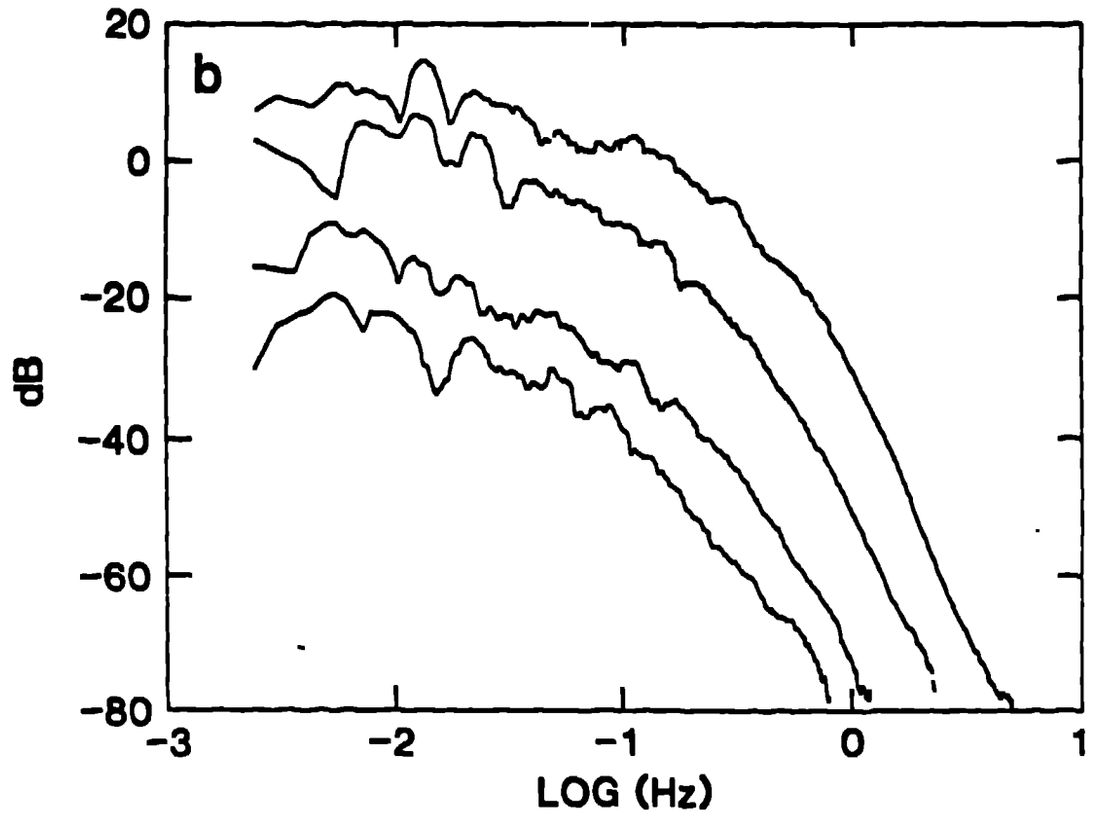
b
20
0
-20
-40
-60
-80
dB
-3
-2
-1
0
1
LOG (Hz)